Science of the Total Environment 954 (2024) 176699

Contents lists available at ScienceDirect

Science of the Total Environment

journal homepage: www.elsevier.com/locate/scitotenv

Feasibility study of electrodialysis as an ammonium reuse process for covering the nitrogen demand of an industrial wastewater treatment plant

Liad Weisz [*,1], Daniela Reif [1], Sascha Weilguni [1], Vanessa Parravicini, Ernis Saracevic, Jörg Krampe, Norbert Kreuzinger

Institute of Water Quality and Resource Management, TU Wien, Vienna, Austria

HIGHLIGHTS

- Investigation of a two-stage ED as an NH_4-N reuse technology from municipal ADLs.
- Stage 1 included 8 sequencing batches, while stage 2 comprised a single batch.
- A maximal concentration of 15 g NH_4-N/L was achieved after both stages.
- The mean specific energy consumption was 12.9 kWh/g NH_4-N.
- An ED side-stream treatment in a model WWTP was beneficial for the energy balance.

GRAPHICAL ABSTRACT

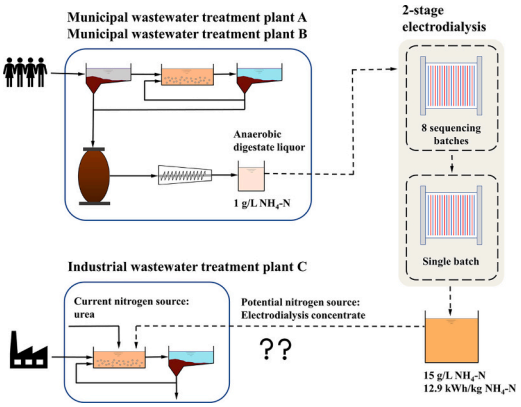

ARTICLE INFO

Keywords:
Electrodialysis
Ammonium recovery
Nutrient recovery
Anaerobic digestate liquor
Desalination

ABSTRACT

Electrodialysis (ED) is a cost-effective membrane technology used is a variety of fields for desalination and concentration. This feasibility study explores the potential of ED as an NH_4-N recovery technology from anaerobic digestate liquor (ADL), and the use of the concentrate as a nitrogen source in an industrial wastewater treatment plant (WWTP). Three neighboring WWTPs were the focus of this study: Two municipal WWTPs A and B, operating anaerobic sludge stabilization, and a pulp & paper WWTP C, utilizing urea as a nitrogen source. Two-stage bench-scale experiments with the municipal ADL from WWTP A and WWTP B were conducted, and performance indicators were determined. A concentration of approximately 10 g NH_4-N/L and 15 g NH_4-N/L was obtained in stages 1 and 2, respectively. The NH_4-N removal was above 85 % in all experiment, while recovery varied between 25 and 95 %. The specific energy consumption (SEC) was on average 12.9 kWh/kg NH_4-N. Moreover, mass and energy balances in a model WWTP demonstrated that an ED side-stream treatment for NH_4-N removal coupled with microfiltration (MF) pre-treatment results in a net energy gain, also without the added benefit of the ED concentrate as a nitrogen source.

* Corresponding author.
E-mail address: liad.weisz@tuwien.ac.at (L. Weisz).
[1] These authors contributed equally to this work and share first authorship.

https://doi.org/10.1016/j.scitotenv.2024.176699
Received 15 June 2024; Received in revised form 28 September 2024; Accepted 1 October 2024
Available online 2 October 2024

1. Introduction

Wastewater treatment using the conventional activated sludge process (CAS) requires specific concentrations of nitrogen and phosphorus to maintain adequate nutrient levels for biomass growth and biological carbon degradation. Conventionally, the ideal influent BOD_5:N:P ratio is known to be 100:5:1 for aerobic treatment (Springer, 1993). However, in municipal wastewater, this ratio is often skewed towards higher nitrogen and phosphorus concentrations relative to BOD_5, necessitating nitrification and denitrification for nitrogen removal, as well as chemical or biological phosphorous elimination.

Industrial wastewater composition typically presents deviations from the above-mentioned ratio due to unique industry-specific components. Specifically, wastewater from the pulp & paper industry is characterized by high organic content and low nitrogen levels. Such nitrogen-deficient wastewater can cause structural degradation of the sludge and bulking by filamentous bacteria, leading to operational challenges (Kocaturk and Erguder, 2016). Consequently, nitrogen-based nutrients such as urea are typically added in wastewater treatment plants (WWTPs) managing this type of wastewater. Urea, a molecule containing a carbonyl group and two primary amines, hydrolyzes to produce CO_2 and two ammonia (NH_3) molecules, which further converts to NH_4-N at pH values typical for biological wastewater treatment. Today, global urea production is dominated by the Bosch-Meiser process, which requires NH_3 and CO_2 as building blocks. The first building block, NH_3, is conventionally produced by the Haber-Bosch process, which is an energy-intensive process running on high temperature and pressure (Xie et al., 2016). The second building block, CO_2, which is typically derived from a high-carbon-footprint source, undergoes a 2-step reaction with NH_3 to produce urea (Mao et al., 2024).

As alternative to technically produced ammonia and urea, municipal WWTPs with anaerobic sludge stabilization could also be considered a nitrogen source. Anaerobic digestion is a widely used stabilization technique, as it reduces the organic content of the sludge and generates biogas, which is mostly used as a source of heat and energy. While dewatering the digested sludge, anaerobic digestate liquor (ADL) is produced, which is rich in NH_4-N due to the hydrolysis of proteins, urea, and nucleic acids from the feed sludge (Tian et al., 2018). Typically, ADL is either recirculated into the main treatment stream for biological treatment and subject to nitrification and denitrification together with the raw inflow, or directed to side-stream treatments. ADL side-stream treatments include i) biological processes such as nitritation and denitratation, as well as deammonification (partial nitritation coupled with anammox), ii) chemical-physical processes such as struvite precipitation, membrane stripping, steam stripping, and air stripping with acid scrubbing (Baumgartner et al., 2022; Chen et al., 2023; Yuan et al., 2016; Zeng et al., 2006).

While the biological processes aim to eliminate nitrogen through the final production of nitrogen gas, N_2, that subsequently cannot be further used, the chemical-physical process can also recover nitrogen for further use. The Sherwood plot for resource recovery depicts the theoretical relationship between the cost of recovering a target material from a waste matrix and its dilution in it. Accordingly, the recovery cost is directly proportional to its dilution (Karakatsanis and Makropoulos, 2022). As municipal ADLs feature the highest NH_4-N concentrations of all wastewater streams (commonly at 1 g NH_4-N/L), NH_4-N recovery may represent an economically viable strategy. In addition to stripping technologies, various technologies have been explored in this regard, including the aforementioned struvite precipitation (Aguilar-Pozo et al., 2023; Pastor et al., 2010), zeolite adsorption (Muscarella et al., 2021; Tokushige and Ryu, 2023), ion exchange (Wirthensohn et al., 2009), and electrodialysis (ED) (Meng et al., 2022).

ED is a cost-effective membrane technology used for desalination and ion recovery from aqueous waste streams (Strathmann, 2010). Due to an alternating arrangement of Anion Exchange Membranes (AEM) and Cation Exchange Membranes (CEM), and the use of direct current (DC), the ED process separates an aqueous solution into an ion-rich concentrate and an ion-deficient diluate.

The driving force for the ion transport is the electric potential difference applied across a series of ion exchange membranes, which causes ions to migrate through the membrane from the diluate stream to the concentrate stream. The electro-migration takes place until the limiting current density (LCD) is reached. This point marks the highest allowable current density at which the ion concentration on the membrane surface drops to zero within the diluate cell (Hyder et al., 2021). At the LCD, water splitting and precipitation take place, which is disadvantageous for the membrane integrity and lifetime. For this reason, prior to desalination, the LCD is typically determined for different sample dilutions (Knežević et al., 2022). Subsequently, the ED process is conducted under dynamic current density control, which adjusts the current density to the diluate electrical conductivity (EC). Moreover, desalination with a dynamic current density offers energetic benefits compared to fixed current density, as lower current densities are required for lower diluate EC, which results in lower power demand.

An operation of a dynamic current density versus fixed current density was investigated by van Linden et al. (2019) for the concentration of a synthetic 1.5 g NH_4^+/L solution in sequencing batch experiments. When operating in a fixed current density control, a concentration factor of 4.5 could be achieved, while a dynamic control achieved a concentration factor of 6.7. Moreover, a fixed current density resulted in a faster increasing concentrate volume, decreasing current efficiency and increasing specific energy consumption (SEC) along the NH_4-N concentration gradient. Conversely, these parameters yielded steadier values when dynamic control was applied.

Another factor that has to be considered in the ED design is the initial volume ratio between diluate and concentrate. When a reverse osmosis concentrate was applied as feed, a volume ratio $V_{diluate}/V_{concentrate}$ of 3:1 resulted in a quicker transport of ions to the concentrate stream compared to a volume ratio of 1:1 (Jiang et al., 2014). Yan et al. (2016) investigated several concentration ratios between 2:1 to 8:1 for the concentration of an ionic liquid. They reported that the experiment with the highest volume ratio of 8:1 resulted in the highest concentration factor, which was however restricted due to a large volume increase of the concentrate.

Commonly, a volume increase of the concentrate is expected during ED due to phenomena of electro-osmosis and forward osmosis, thereby limiting the reachable concentration factor. Electro-osmosis is the coupled transfer of water molecules with the charged species, and is linked to their hydration number (Han et al., 2015). Forward osmosis is the transfer of water due to increasing osmotic pressure gradient between the diluate and concentrate streams. While the former is directly linked with ion transfer, the latter is expected to play an increasing role at an increasing concentrate concentration (Liu and She, 2022).

The ED technology has demonstrated its feasibility for the desalination of brackish water, being the second most utilized technology in this field after reverse osmosis (Ortiz et al., 2005; Patel et al., 2021; Tsiakis and Papageorgiou, 2005). In addition, it has been applied for the concentration of fermentation by-products (Knežević et al., 2023; Papadopoulou et al., 2023), for the desalination of secondary effluents (Albornoz et al., 2019; Liu et al., 2017), and for the recycling of industrial process streams (Benvenuti et al., 2017; Bernardes et al., 2000; Scarazzato et al., 2018). In the context of NH_4-N removal and recovery from ADL, literature review reveals that although the ED-based approach might be technically suitable, it bears limitations concerning the achievable concentration factors and percent of recovery. Ward et al. (2018) concentrated anaerobic centrate through a pilot scale ED, which resulted in an NH_4-N concentration factor of 8 and a current efficiency for ion transport of 76 % ± 2 %. The SEC was reported as 4.9 ± 1.5 kWh/kg NH_4-N, while the recovery amounted to 23 %. Mondor et al. (2008) concentrated NH_4-N from swine manure, suggesting that under their experiment conditions a maximum of 16 g/L could be obtained. Wang et al. (2015) applied ED for the recovery of NH_4-N and PO_4-P from

ADL, obtaining removal ratios of 95.8 % – 100 % and 86.1 % – 94.4 %, respectively. Considering the range of concentration factors and recoveries discussed in the literature, further optimization work is needed before the ED technology can be implemented on a large scale as a side-stream treatment for ADL.

When considering NH_4-N removal from ADL in WWTPs with main-stream ADL recirculation, the effect of the resulting lower nitrogen load on the activated sludge should be accounted for as well. In the CAS process, the incoming NH_4-N undergoes a biological two-step nitrification, in which it is oxidized to nitrite (NO_2-N) and subsequently, to nitrate (NO_3-N) under aerobic conditions. Then, NO_3-N is reduced to N_2 with organic compounds serving as an electron donor by heterotrophic denitrification. The nitrification step consumes 4.33 kg O_2 per kg NO_3-N produced, while the denitrification step yields 2.86 kg O_2 per kg NO_3-N under anoxic conditions. In WWTPs that operate anaerobic sludge stabilization, the nitrogen load from the recirculated ADL typically makes up to 15 % – 20 % of the incoming nitrogen load. For denitrification, however, a lower nitrogen load would result in an excess of COD than stoichiometrically needed for NO_3-N reduction, which consequently requires additional oxygen for its oxidation. Alternatively, the excess COD could be removed already in the primary sedimentation tank as primary sludge (PS) and diverted into the anaerobic digestion tank, thus favorably increasing the production of biogas.

Given the high energy demand for the production of ammonia and urea, along with price fluctuations in the energy industry, which are driven by geopolitical factors, fertilizer prices are directly impacted. Therefore, harvesting nitrogen fertilizer from a nearby municipal WWTP would decrease the dependency on the global urea market, and would potentially improve the energy balance of the municipal WWTP at the same time. Equally important, repurposing one industry's waste stream as a value stream for a neighboring industry reduces the need for long-distance transport due to off-site production, thereby aligning well with circular economy principles and current legislation (Gherghel et al., 2019).

1.1. Objective

In this feasibility study, we investigated the use of ED as a technology for NH_4-N recovery from the ADLs of two municipal WWTPs, named A and B. WWTP C, which lies in the vicinity of both municipal WWTPs, is an industrial pulp & paper plant, currently utilizing externally purchased urea as a nitrogen source to support activated sludge growth. To achieve this, bench-scale experiments were conducted and different performance indicators of the ED technology were evaluated. In order to estimate the membrane area required to generate a daily NH_4-N load and thus meet the demand of WWTP C, the NH_4-N flux density was determined in all batches. In addition, the volume increase of the concentrate was accounted for, as it directly impacts the achievable concentration factor and the feasibility of transporting the concentrate. Moreover, NH_4-N current efficiency and the SEC were determined in order to examine the overall energetic efficiency of the process. Apart from the recovery aspect along with the potential benefit it holds to reuse the locally produced NH_4-N, the energetic aspect of NH_4-N removal from ADL was analyzed on a model WWTP by conducting mass and energy balances.

Fig. 1 illustrates the proposed integration of the ED process in a municipal WWTP. The grey rectangles depict a municipal WWTP with CAS process and anaerobic sludge stabilization, similar to WWTPs A and B. After anaerobic digestion of the PS and waste activated sludge (WAS), the digested sludge is dewatered by using a centrifuge before being disposed of. As previously mentioned, the ADL is typically recirculated to the main biological treatment stage or alternatively directed to a side-stream treatment. In the proposed scheme, the ADL undergoes a side-stream treatment that includes pre-treatment through microfiltration

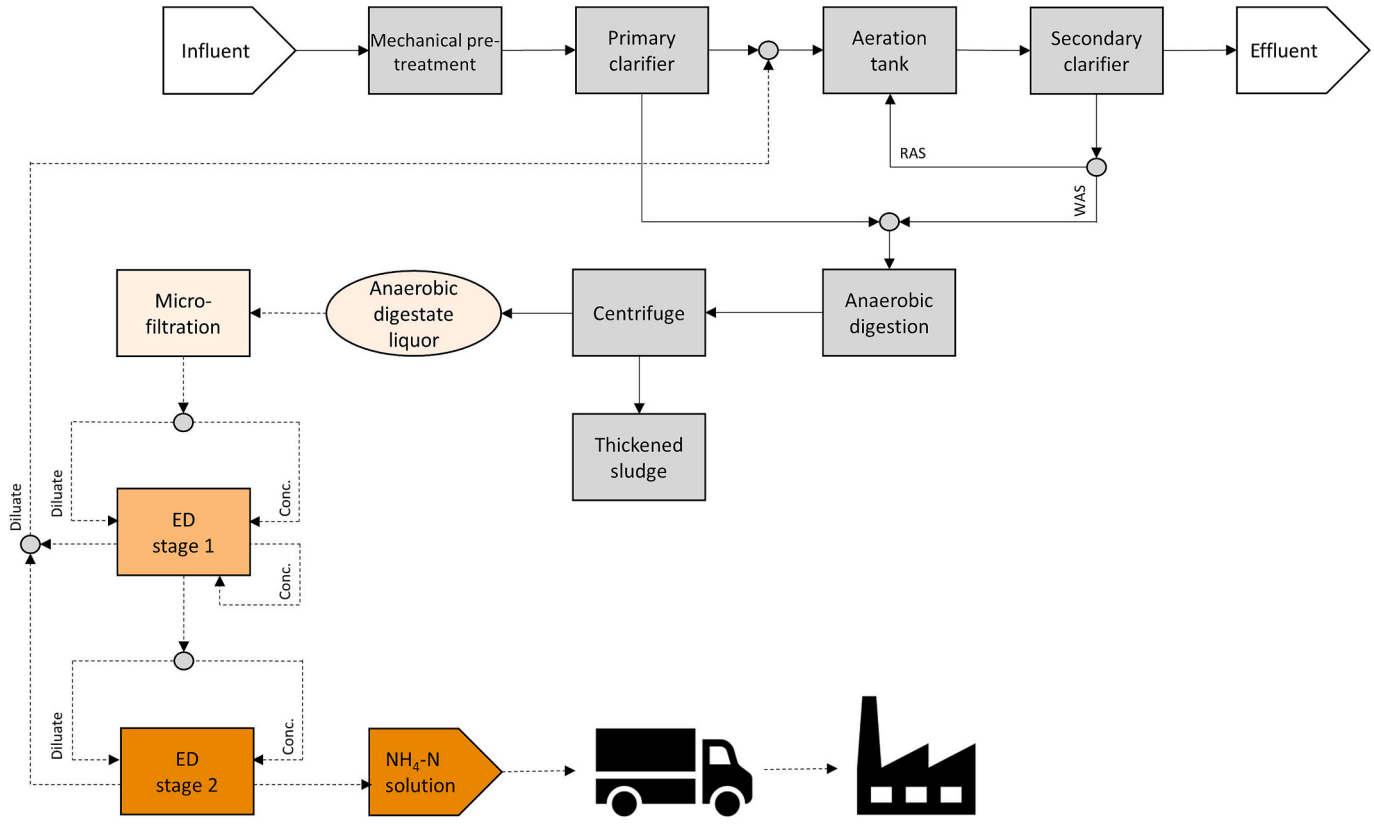

Fig. 1. Generic scheme of a municipal WWTP operating CAS (continuous lines), and proposed scheme for the preparation of an NH_4-N solution by ED for the usage as NH_4-N source in an industrial WWTP (dashed lines).

(MF), followed by two ED concentration stages.

According to our approach, eight sequencing batch experiments were conducted in stage 1 of the ED process, where the desalinated ADL diluate was replaced with fresh ADL after each batch, allowing for continuous concentrate concentration. To minimize forward osmosis and back-diffusion of NH_4-N at an increasing concentration gradient, while significantly increasing the amount of transportable NH_4-N, the concentrate from stage 1 was split into diluate and concentrate for a further batch experiment in stage 2. Ultimately, the obtained NH_4-N solution is available for transport to WWTP C.

2. Materials and methods

2.1. WWTP and ADL characterization

WWTP A treats an approximate influent wastewater flowrate of 7000 m^3/d and is designed for 70,000 PE (population equivalents), while WWTP B treats approximately 5000 m^3/d and is designed for 25,000 PE. Both municipal WWTPs incorporate a mechanical treatment stage, a biological treatment stage with nitrification and denitrification, and a chemical treatment for phosphorous removal. The combined sludge from the PS and WAS is dewatered and undergoes mesophilic anaerobic digestion, and the produced biogas is converted to energy and heat via combined heat and power combustion engines (CHP). The digested sludge is dewatered, and the arising ADL is returned to the biological treatment stage.

The industrial WWTP C is located at a large pulp & paper manufacturing facility with an annual capacity of 460,000 tons pulp and 200,000 tons paper. It doses a daily mean of 943 kg urea/d, equivalent to 440 kg urea-N/d into the activated sludge tank (AST). In the years 2020–2022, WWTPs A and B generated a mean NH_4-N load of 141 kg NH_4-N/d and 25 kg NH_4-N/d, respectively. The ADL inflow, average NH_4-N concentrations and average NH_4-N loads of both municipal WWTPs are listed in Table 1.

For the ED experiments, ADL samples were taken from both municipal WWTPs, and analyzed for PO_4-P and NH_4-N, ions, as well as pH and electrical conductivity (EC). A chemical characterization of the ADLs is provided in Table 2.

2.2. Experimental set-up

The experiments were conducted with the ED unit PCCell ED 64–004 (Germany), consisting of a 10-cell pair stack containing 10 AEM and 9 CEM, each having an effective membrane area of 64 cm^2. Fumasep FKS-PET-130 and Fumasep FAS-PET-130 were applied as AEM and CEM, both manufactured by Fumatech (Germany). The stack included polyethylene/silicone spacers with a thickness of 0.45 mm. The electrodes used were Pt/Ir-coated titanium anode and V4A steel cathode, with a maximal current of 5 A, and a maximal voltage of 30 V. The diluate and concentrate streams were recirculated through the ED unit at 15 L/h (linear velocity of 0.012 m/s) while constant water cooling was maintained in the double-walled feed tanks. A 0.25 M Na_2SO_4 electrode-rinse solution was used at a flowrate of 120 L/h. The EC and temperature in both streams, and the pH of the diluate, were continuously monitored and logged automatically. The experimental set-up is illustrated in Fig. S6 of the Supplementary Material.

Table 1
ADL inflow, NH_4-N concentration and NH_4-N load in WWTPs A and B (mean values).

Year	WWTP A			WWTP B		
	ADL inflow	NH_4-N concentration	NH_4-N load	ADL inflow	NH_4-N concentration	NH_4-N load
	m^3/d	mg/L	kg/d	m^3/d	mg/L	kg/d
2020	89	1493	142	30	866	26
2021	100	1533	153	29	838	24
2022	95	1445	129	27	886	24

2.3. LCD experiments

The LCD was determined in duplicates for both ADLs from WWTP A and B with the method suggested by Cowan & Brown (Knežević et al., 2022). Accordingly, resistance-reciprocal current density curves were drawn and the inflection point for each curve was determined, as shown in Figs. S1 and S2. Experimentally, the current was initially set to 5 A, corresponding to a current density of 78 A/m^2, and the voltage was increased in a 2-V step from 5 V to 29 V. For each step, a time interval of 90 s was selected. The LCD was determined for three dilution factors of 1, 2 and 3 by diluting the ADL with milli-Q water. For each ADL, a regression line between LCD-EC was derived, as depicted in Fig. S3. The concentration experiments for the ADLs from WWTP A and B (ADL A and ADL B) were performed with a current density (CD) calculated according to Eq. 1, with a safety factor (SF) of 0.8. The coefficients for ADL A were 23.73 for "m" and 9.76 for "b", while for ADL B, the coefficients were 19.26 for "m" and 8.86 for "b". The correlation between the CD with the obtained diluate EC shows that once the diluate EC was reached, the CD was reduced accordingly in a stepwise manner.

$$CD = (m \bullet EC_{diluate} + b) \bullet SF \quad (1)$$

2.4. Concentration experiments

Two identical experiments were conducted for each ADL. Prior to the first experiment of a given ADL, the membranes and spacers were cleaned with running tap water, whereas in the subsequent second experiment, no cleaning procedure was included. Each ED experiment consisted of two stages. Stage 1 included 8 sequencing batch experiments, in which the concentrate was continuously concentrated by replacing the desalinated diluates with a fresh feed. The first batch in stage 1 experiment started with 1.5 L diluate and 0.5 L concentrate, whereas the concentrate was maintained for the subsequent batches. Each batch in the concentration experiment was aborted when the diluate EC reached a value of 0.5 mS/cm, or when no further reduction below 2 mS/cm was reached.

Stage 2 included a single batch, in which 66.6 vol-% of the stage 1 concentrate, obtained after 8 sequencing batches, was filled in the diluate chamber, and 33.3 vol-% was filled in the concentrate chamber. Therefore, the volume ratio $V_{diluate}/V_{concentrate}$ of 3:1 was kept as in the first batch of stage 1. Desalination of stage 2 diluate was carried out until an EC of 10 mS/cm was reached. After each batch of stages 1 and 2, 10 mL sample was taken for the chemical analysis of NH_4-N and PO_4-P.

The experiments were labeled using a three-part code: the first part, either "A" or "B," indicated the ADL from the corresponding municipal WWTP. The second part, "1" or "2," denoted the experiment number (first or second). The third part, again "1" or "2," referred to the specific stage within the experiment.

2.5. Chemical analysis

The samples were analyzed for the parameters NH_4-N and PO_4-P with continuous flow analysis and photometrical detection (Skalar, Netherlands) according to DIN EN ISO 6878 and DIN EN ISO 11732 standards, respectively. It should be noted that although NH_4-N is referred to as the measured species throughout this study, TAN (total ammonium nitrogen – encompassing both NH_4-N and NH_3-N) was in fact measured.

2.6. Data analysis and calculations

The following ED performance indicators were analyzed: NH_4-N

Table 2
Characteristics of the ADLs.

Parameter	PO_4-P	NH_4-N	Cl	SO_4	K	Ca	Mg	pH	EC
Unit	mg/L	mg/L	mg/L	mg/L	mg/L	mg/L	mg/L	–	mS/cm
WWTP A	34.1	991.5	168.1	248	505	2025	0	7.8	7650
WWTP B	49.4	833.7	279.8	42.9	0	849	0	8.7	8380

current efficiency, SEC, concentrate volume increase, and NH_4-N flux density. To assess the difference between experiments A11 and A21, as well as between B11 and B21, a student's independent *t*-test was conducted with a significance level of 0.001 ($P < 0.001$). Furthermore, a model WWTP was applied to calculate the PE-specific energy demand by introducing ED as a side-stream treatment.

The current efficiency is defined as the ratio between the charge transferred by ions permeating the membrane divided by the electrical charge transferred by the electrodes. The calculation of the current efficiency for the transport of NH_4-N was performed according to Eq. 2 for each batch experiment.

$$\eta_{NH_4-N} = \frac{z \bullet F \bullet \Delta n_{NH_4-N}}{N \bullet \sum (I \bullet \Delta t)} \bullet 100 \quad (2)$$

where η_{NH_4-N} is the NH_4-N current efficiency (in percent), z is the ion valence (unitless), F is the Faradays constant (C/mol), Δn_{NH_4-N} is the number of moles of NH_4-N transferred to the concentrate stream (mol), N is the number of cell pairs (unitless), I is the electrical current (A) and Δt is the experiment time (s).

The SEC of the ED unit, normalized to the recovered NH_4-N after each batch, was determined for each batch experiment according to Eq. 3.

$$E_{NH_4-N,ED} = \frac{\sum U \bullet I \bullet \Delta t}{\Delta m_{NH_4-N}} \quad (3)$$

Where $E_{NH_4-N,ED}$ is the SEC of the ED unit (kWh/kg NH_4-N), U is the voltage (V), I is the current density (A), Δt is the experiment duration, and Δm_{NH_4-N} is the mass of NH_4-N transferred to the concentrate stream (kg).

The SEC of the electrolyte, diluate and concentrate pumps, normalized to the recovered NH_4-N after each stage, was determined for each stage according to Eq. 4.

$$E_{NH_4-N,pump} = \frac{\sum \dot{V} \bullet \Delta p \bullet \Delta t}{\Delta m_{NH_4-N}} \quad (4)$$

Where $E_{NH_4-N,pump}$ is the SEC of pumping (kWh/kg NH_4-N), $\dot{V}$ is the volumetric flowrate (m^3/s), and Δp is the pressure drop (Pa). To calculate the SEC of pumping, a pressure drop of 0.5 bar (50,000 Pa) was assumed.

The volume increase of the concentrate was determined in relation to the previously conducted batch experiment, as shown in Eq. 5. In stage 2, the volume increase was determined in relation to the eighth batch experiment from stage 1.

$$V_{Conc,i+1} = \frac{V_{Conc,i+1} - V_{Conc,i}}{V_{Conc,i+1}} \bullet 100 \quad (5)$$

3. Results

3.1. NH_4-N concentrations and mass balance

Figs. 2 and 3 depict the change of EC and NH_4-N concentration with the experiment duration. In experiment A11, the diluate EC could be reduced to 0.5 mS/cm in every batch experiment, whereas in experiments A21, B11 and B21 such an EC decrease could be achieved only in the first batch experiments, and the consecutive experiments were aborted at 2 mS/cm. In experiment A11, the EC of ADL A concentrate increased from 10.2 mS/cm to 69.0 mS/cm, and from 7.7 to 60.4 mS/cm in experiment A21. The largest EC increase was evident in the first batch experiments, and the increase plateaued with increasing concentration gradient. After the first batches of experiments A11 and A21, ΔEC amounted to 18.5 mS/cm and 14.7 mS/cm, while it decreased to 4.3 mS/cm and 4.8 mS/cm after the eighth batch experiments. A similar trend was observed for the ADL B concentrate (experiments B11 and B21), which showed a large ΔEC in the start, which leveled off in the further batches.

In stage 2, the EC of WWTP A concentrate steeply increased from 69.0 mS/cm to 94.5 mS/cm, and from 60.4 mS/cm to 96.7 mS/cm in experiments A12 and A22, respectively. This was accompanied by a corresponding EC decrease in the diluate, reaching an EC of 10 mS/cm. As can be shown in Fig. 2b, a similar trend of EC increase was observed in ADL B concentrate (experiments B12 and B22). ΔEC of stage 2 amounted to 25.5 mS/cm and 36.3 mS/cm in both experiment A12 and A22, and to 35.2 mS/cm and 28.6 mS/cm in experiment B12 and B22.

A comparison of the EC and the obtained NH_4-N concentration curves reveals that both municipal ADLs follow the same trend. Unsurprisingly, the high ammonium concentration of the ADL is a large contributor for the EC, as seen in Fig. 3. NH_4-N concentration increased from 1.3 g/L to 10.4 g/L in experiment A11, and then to 15.2 g/L in experiment A12. In experiment A21, a lower NH_4-N concentration was reached, in line with the lowered EC, which was attributed to the lack of an additional cleaning step in this experiment. NH_4-N concentration increased from 0.85 g/L to 8.2 g/L in experiment B11, and from 8.2 g/L to 14.9 g/L in experiment B12. Similar results were obtained in experiments B21 and B22, although the experiment duration was longer in the former (15.1 h versus 12.5 h).

Table 3 lists the percent of NH_4-N removal, recovery and loss observed in all experiments. In both municipal ADLs, NH_4-N removal above 85 % ± 8 % and 88 % was obtained in stages 1 and 2, respectively. From the total NH_4-N removed, 64 % ± 14 % and 75 % ± 16 % could be transferred to the concentrate in experiments A11 and A21. In stage 2, 25 % and 95 % could be transferred to the concentrate in experiments A12 and A22, respectively. Despite the large difference, both experiments yielded a final concentrate concentration of circa 15 g NH_4-N/L. It is therefore plausible that under the operating conditions, NH_4-N could not further be concentrated, as shown in Fig. 2 by the plateauing in stage 2 towards the end of the experiments. More comparable results were obtained in experiments B1 and B2, with an NH_4-N recovery of approximately 70 % in stage 1, and a lower NH_4-N recovery in stage 2, lying between 40 % and 47 %.

3.2. NH_4-N flux density and concentrate volume

The increase in concentrate volume is illustrated in Fig. 4a and b for both municipal ADLs. In experiment A11 and A21, apart from the second batch of experiment A11 and the seventh batch of experiment A21, a slight and steady increase of the concentrate volume was observed. In experiment A11, it increased from 1.1 % in the first batch to 8.5 % in the eighth batch. Since the volume increase rose steadily at increasing concentrate concentration, this suggests that in addition to electro-osmosis, forward osmosis was as well present. In experiments B11 and B21, the concentrate showed a constant volumetric increase of approximately 5 %, for which electro-osmosis was interpreted as the most relevant mechanism. In the experiments with ADL B, NH_4-N could be transferred to the concentrate at a similar percentage in stage 1

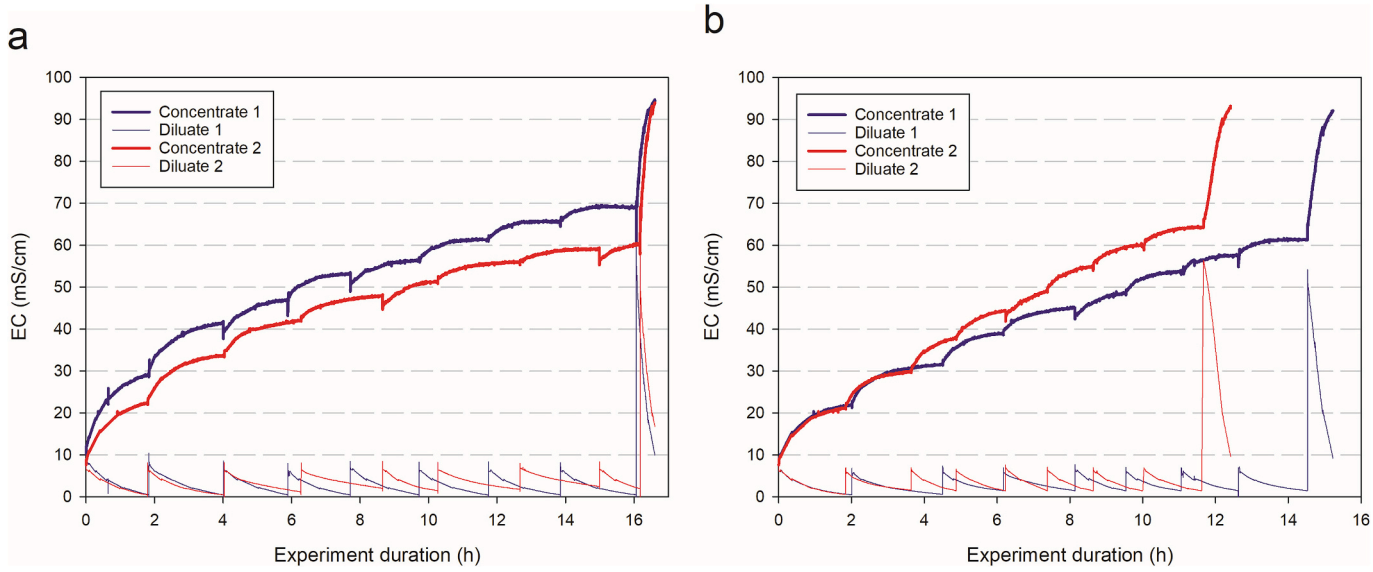

Fig. 2. The EC in dependence of the experiment duration in ED experiments with ADL A (a) and ADL B (b). The steep EC increase marks the beginning of stage 2.

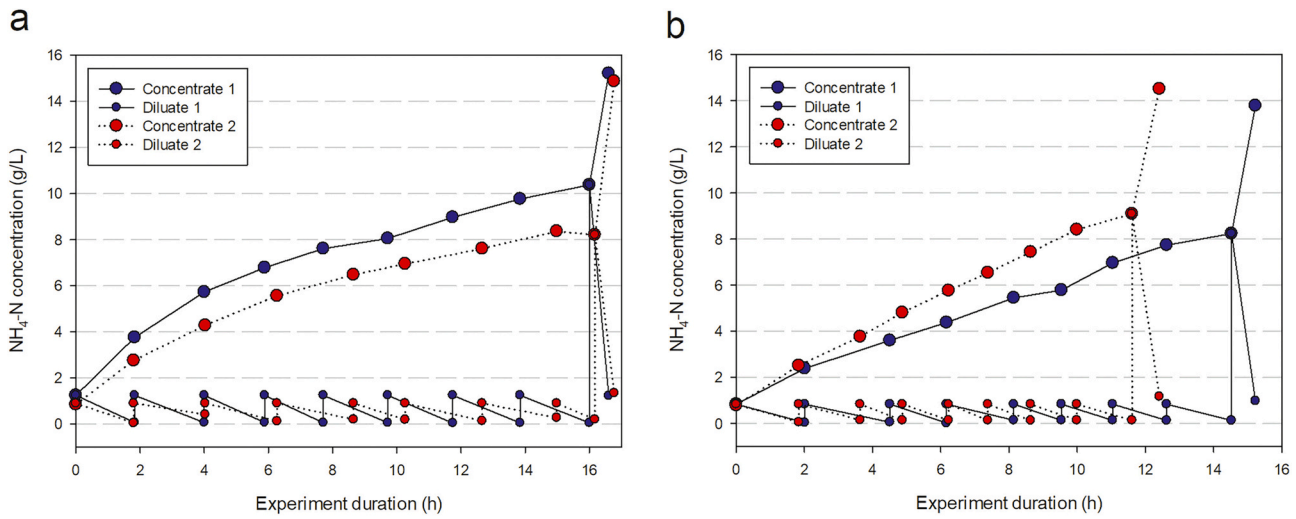

Fig. 3. The NH_4-N concentration in dependence of the experiment duration in ED experiments with ADL A (a) and ADL B (b). The steep increase in NH_4-N concentration marks the beginning of stage 2.

Table 3
Mass balance of all experiments. The percent of NH_4-N removed is normalized to the NH_4-N concentration in the feed. The percent of NH_4-N recovered and lost is normalized to the NH_4-N removed.

	Experiment A1		Experiment A2		Experiment B1		Experiment B2	
	Stage 1	Stage 2	Stage 1	Stage 2	Stage 1	Stage 2	Stage 1	Stage 2
NH_4-N removed (mg)	1505 ± 163	5061	1153 ± 103	3722	1088 ± 59	3773	1086 ± 60	3686
NH_4-N removed (%)	95 ± 1	89	85 ± 8	89	87 ± 5	88	87 ± 5	88
NH_4-N recovered (mg)	954 ± 219	1255	739 ± 400	3546	761 ± 191	1496	754 ± 110	1735
NH_4-N recovered (%)	64 ± 14	25	75 ± 16	95	70 ± 17	40	69 ± 9	47
NH_4-N loss (mg)	552 ± 219	3806	292 ± 181	176	327 ± 192	2278	332 ± 98	1951
NH_4-N loss (%)	37 ± 14	75	25 ± 16	5	30 ± 18	60	31 ± 9	53

batches (70 % ± 17 % in experiment B11 and 69 % ± 9 % in experiment B21).

Stage 2 marked the highest volume increase in relation to the eighth batch of stage 1, with 34.5 % and 32.5 % in experiment A12 and A22, and 23.5 % in experiments B12 and B22. As the feed in stage 2 was 10-times more concentrated than in the first batch of stage 1, this results in a fast NH_4-N electro-migration and a volume increase owed initially to electro-osmosis. At the end of stage 2, the slight plateau in the EC curve suggests the beginning of NH_4-N back-diffusion or forward osmosis.

As seen in Fig. 5, the NH_4-N flux density remained consistent throughout stage 1 in both experiments A and B, with values averaging approximately 0.5 mol/(m^2·h). Similar to the increase in concentrate volume, there was a significant increase of the flux density in stage 2, indicating the importance of electro-osmosis to the concentrate volume

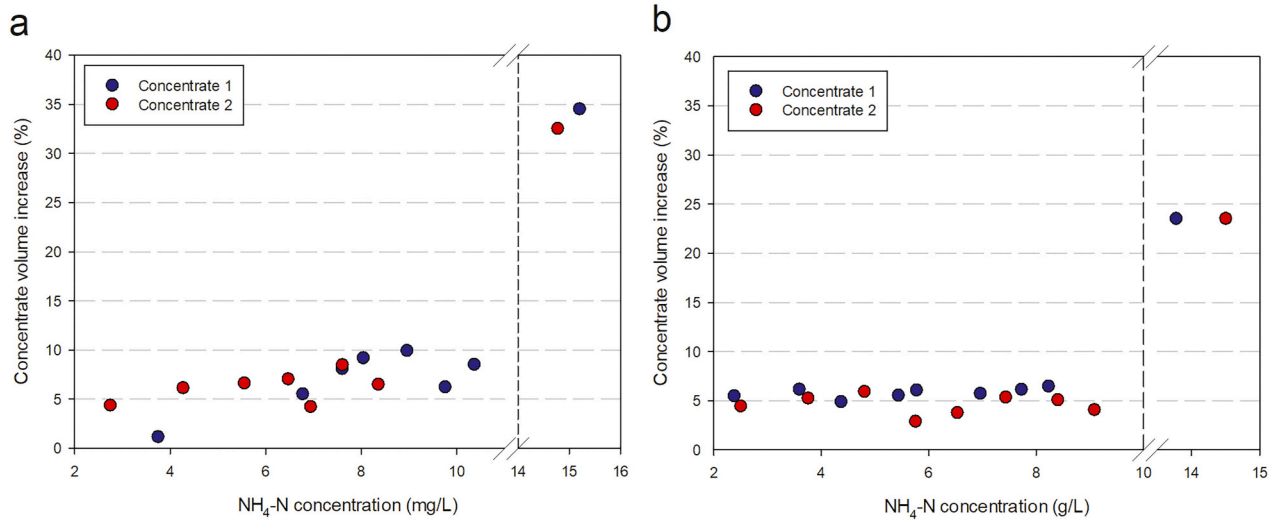

Fig. 4. The percentual concentrate volume increase in dependence of the NH_4-N concentration in ED experiments with ADL A (a) and ADL B (b). Left to vertical dashed line: Stage 1; Right to vertical dashed line: Stage 2.

increase. In stage 2, the NH_4-N flux density increased to 6.5 and 6.6 mol/(m^2·h) in experiments A12 and A22, and to 2.8 and 3.1 mol/(m^2·h) in experiments B12 and B22.

There was no statistically significant difference in concentrate volume increase or NH_4-N flux density between experiments A11 and A21, or between B11 and B21 ($P < 0.001$), showing that a cleaning step did not significantly impact the obtainable performance indicators.

3.3. NH_4-N current efficiency and specific energy consumption

The NH_4-N current efficiency varied between 23.3 %–37.7 %, and 18.9 %–32.6 % in experiment A11 and A21, respectively, as illustrated in Fig. 6a. Since the removed NH_4-N could not be recovered in the eighth batch of experiment A21, as also shown by the negative flux density, the NH_4-N current efficiency was negative in this batch. In experiments B11 and B21, the NH_4-N current efficiency ranged between 20.1 %–45.5 % and between 26.9 %–41.2 %, respectively, as shown in Fig. 6b. In stage 2, the NH_4-N current efficiency increased slightly to 46.5 % and 54.2 % in experiment A21 and A22 compared to stage 1, and remained at a similar range as stage 1 in experiments B21 and B22 with 31.7 % and 31.8 %. In both ADLs, no statistically significant difference regarding the effect of the cleaning step on the NH_4-N current efficiency was observed ($P < 0.001$).

The SEC versus NH_4-N concentration is depicted in Fig. 7a and b. In experiment A11, the SEC varied between 5 and 12 kWh/kg NH_4-N, and reached 19 kWh/kg NH_4-N in experiment A12. In experiment A21, the SEC had an increasing trend from 7 to 21 kWh/kg NH_4-N, and declined to 8.5 kWh/kg NH_4-N in experiment A22. Due to NH_4-N loss in the eighth batch, the SEC in that batch was −33 kWh/kg NH_4-N (not shown in the plot). A summary of the SEC values obtained in each municipal ADL at each stage as well as for both the ED unit and pumping is provided in Table 4.

Lower SEC values were obtained in experiment A11 compared to experiment A21, which were attributed to membrane cleaning. The difference between the SEC values obtained in these experiments was statistically significant ($P < 0.001$). In contrast, the opposite trend was observed in experiments A21 and A22. The significantly lower SEC values obtained in experiment A22 were achieved due to the lower NH_4-N concentration obtained in experiment A21 compared to experiment A11 (see Fig. 3a), which enabled a greater NH_4-N transfer at a similar

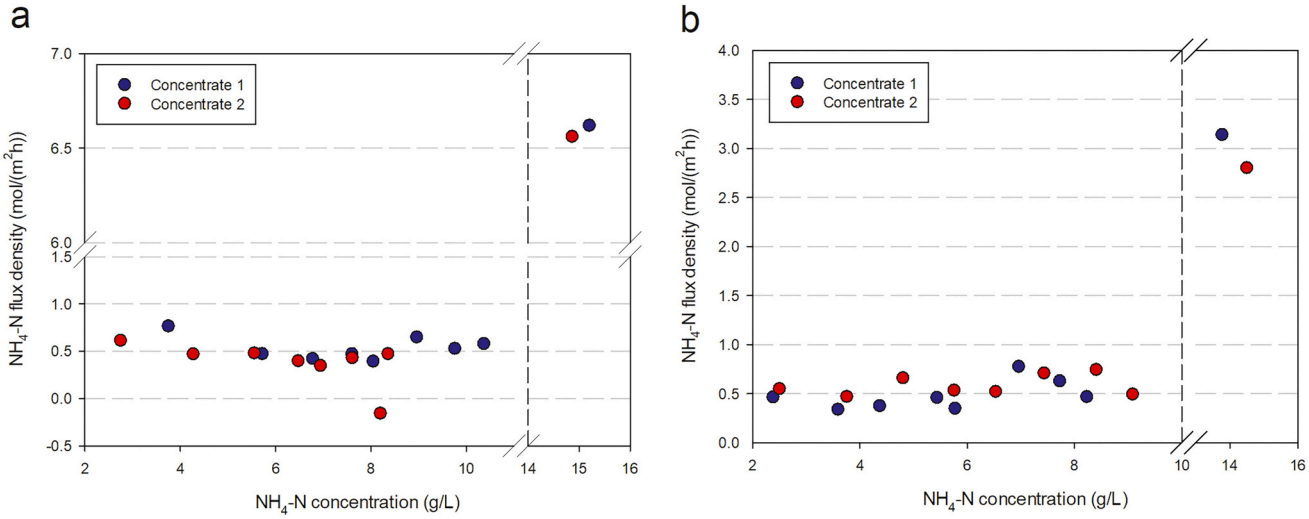

Fig. 5. NH_4-N flux density in dependence of the NH_4-N concentration in ED experiments with ADL A (a) and ADL B (b). Left to vertical dashed line: Stage 1; Right to vertical dashed line: Stage 2.

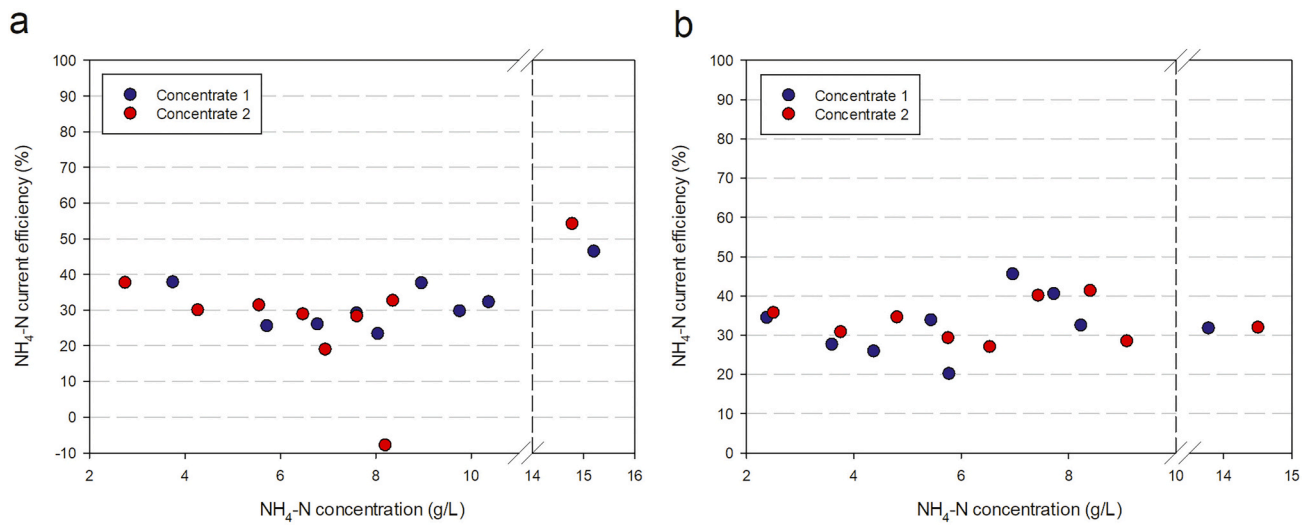

Fig. 6. The percentual NH_4-N current efficiency in dependence of the NH_4-N concentration in ED experiments with ADL A (a) and ADL B (b). Left to vertical dashed line: Stage 1; Right to vertical dashed line: Stage 2.

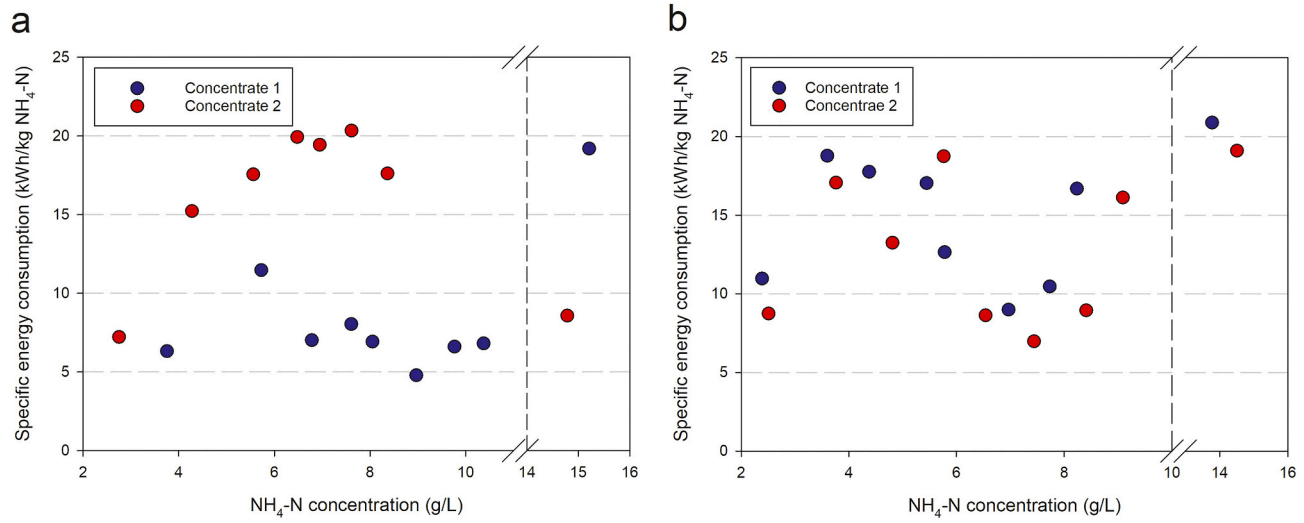

Fig. 7. The SEC in dependence of the NH_4-N concentration in ED experiments with ADL A (a) and ADL B (b). Left to vertical dashed line: Stage 1; Right to vertical dashed line: Stage 2.

time interval and concentrate volume increase, until a concentration of approximately 15 g/L was reached.

In comparison to ADL A, the experiments with ADL B showed in both stages similar trends, and no effect of membrane cleaning on the SEC was apparent ($P < 0.001$). This could be linked to the lower Ca^{2+} concentration in ADL B (849 mg/L) compared to the ADL A (2025 mg/L), which potentially resulted in less scaling on the membrane surface, and thus in an improved ionic flux. However, both experiments with ADL B exhibit high fluctuations along the NH_4-N concentration gradient.

As shown in Table 4, the SEC for pumping was negligible compared to the SEC for the ED unit. Considering the SEC for both the ED unit and the pumps, a mean total SEC for NH_4-N recovery amounted to 11.7 ± 3.5 kWh/kg NH_4-N and 14.1 ± 1.0 kWh/kg NH_4-N in the experiments with ADLs A and B, respectively. While the SEC in stage 2 was generally larger than stage 1 due to the larger NH_4-N concentration in the diluate, the overall effect on the total SEC was low due to the short experiment duration.

Table 4
SEC for NH_4-N recovery (in kWh/kg NH_4-N).

	Experiment A1		Experiment A2		Experiment B1		Experiment B2	
	Stage 1	Stage 2	Stage 1	Stage 2	Stage 1	Stage 2	Stage 1	Stage 2
SEC ED	7.41	8.58	16.64	8.58	12.93	20.87	11.28	19.33
SEC ED total	8.96		13.76		14.41		13.01	
SEC pumps	0.28	0.02	0.37	0.03	0.38	0.03	0.37	0.03
SEC pumps total	0.3		0.4		0.41		0.4	
SEC total	9.26		14.16		14.82		13.41	

4. Discussion

In the ADLs of both WWTPs, a concentration of approximately 10 g NH_4-N/L could be obtained in stage 1, and 15 g NH_4-N/L in stage 2. This corresponds to a mean recovery of 70 % and 50 % in these stages, respectively. A concentration of 15 g/L could be achieved after 16.5 h for ADL A, and 12–15 h for ADL B. In stage 1, the increase in NH_4-N concentration generally plateaued in every sequencing batch, which was attributed to the increasing concentration gradient, resulting in water influx from the diluate stream and in an increase of concentrate volume. In stage 2, a sharp concentration increase could be achieved, owing to the high NH_4-N mass in the diluate chamber given the high initial concentration and the selected volume ratio $V_{diluate}/V_{concentrate}$ of 3:1. Moreover, the short contact time between the recirculating diluate and concentrate streams in stage 2, in comparison to stage 1 batches, helped counteract back-diffusion and forward osmosis.

Given the mean NH_4-N loads of 141 and 25 kg NH_4-N/d in ADL A and B, respectively, and the nitrogen demand of WWTP C with 440 kg urea-N/day, the daily nitrogen loads of the municipal WWTPs are not sufficient for covering the nitrogen demand of WWTP C. For this purpose, a larger WWTP with accordingly higher ADL nitrogen load is required. As aforementioned, the NH_4-N fraction of recirculated ADL in WWTPs with anaerobic sludge stabilization accounts for 15 %–20 % of the influent NH_4-N. For a large municipal WWTP operating anaerobic sludge stabilization with a specific nitrogen load of 8 g N/(PE·d), of which 15 % is fed by the ADL, this results in 1.2 g NH_4-N/(PE·d), which can be recovered from the ADL. To meet the demand of 440 kg urea-N/d required for treating the industrial wastewater from the large pulp & paper factory, a WWTP >300,000 PE is required.

Considering SEC, the Haber-Bosch process is stated to consume 9.7–13.9 kWh/kg NH_3-N (Ward et al., 2018; Xie et al., 2016), whereas the proposed ED technology consumes a mean of 12.9 kWh/kg NH_4-N in all conducted experiments. In ADL A and B, the SEC was 11.3 ± 3.4 kWh/kg NH_4-N and 13.7 ± 1.0 kWh/kg NH_4-N, respectively, whereas the SEC for pumping was negligible compared to the ED unit. As aforementioned, the Bosch-Meiser process for urea production requires an additional step following NH_3 production, in which two NH_3 molecules react with one CO_2 molecule to initially form ammonium carbamate, which is then converted into urea. The latter process is reported to consume 16.2–17.8 kWh/kg urea-N (Rossi et al., 2022; Shi et al., 2020). Although the SEC of ED appears to lie at the same range as for conventional ammonia production and at a lower range than conventional urea production, all three processes utilize different energy inputs. While ED relies on electrical energy, which can be decarbonized based on the primary energy sources used in its production, the other two process predominantly rely on thermal energy, with fossil sources serving both as feedstock and fuel. Therefore, the primary energy sources used in all these technologies should be examined and a conversion factor between the energy inputs should be considered when comparing these processes energetically.

Considering the two subsequent experiments applied for each ADL, a priorly cleaned ED unit was identified as more energy-efficient when ADL A was applied, suggesting that fouling and/or scaling might have hindered NH_4-N removal and recovery in the second experiment. Because the dissolved organic matter (DOM) is usually negatively charged and possesses a larger molecular size compared to small inorganic ions, it might get trapped at the surface of the internal pores of the AEM during the transport process, which results in fouling (Wang et al., 2022). Additionally, scaling might also set in considering the high initial Ca^{2+} concentration of the ADLs at a pH of approximately 8. Further improvement of SEC can be achieved by reducing the percent of NH_4-N removal (and consequently NH_4-N recovery) for each batch, which would reduce the voltage increase observed at lower diluate concentrations. Meng et al. (2022) applied electro-ion substitution modified ED (EIS-ED) for NH_4-N recovery from digested sludge centrate with a recovery of 70 %. This membrane technique was used to reduce fouling and scaling on the AEM by introducing the feed between two CEM, reaching a SEC of 2.03 kWh/kg NH_4-N.

The membrane area required to produce a daily NH_4-N load for WWTP C was estimated based on the molar flux densities observed in all experiments, without accounting for upscaling considerations. In stage 1 experiments, a mean flux density of 0.5 mol/(m^2·h) was observed in the ADLs from both municipal WWTPs, necessitating an active membrane area of 2620 m^2. In stage 2, generally higher flux densities were recorded. Specifically, for ADL A, the mean flux density was 6.6 mol/(m^2·h), resulting in a required membrane area of 199 m^2 in this stage. For ADL B, with a mean flux density of 3 mol/(m^2·h), the required membrane area would be 437 m^2. Therefore, stage 1 is the limiting factor as it requires the largest membrane area.

For a commercialized industrial-scale ED unit with a membrane active area of 0.4 m^2 and maximally 1200 membranes per unit, this results in a total active area of 480 m^2 per unit. Such an active membrane area is sufficient for NH_4-N recovery in stage 2, while 6 units in a parallel operation would be required in stage 1. In practical terms, a parallel operation would increase the capital costs for the process equipment, as additional ED cell units, pumps, pipelines and valves would be required, as well as additional space and higher chemical demand for the electrode rinse solution, which overall increases operational complexity. Consequently, this necessitates further optimization work to increase NH_4-N flux density, improve its recovery and counteract its loss. Applying an anion-exchange end membrane (AEEM) instead of a cation-exchange end membrane (CEEM) for example might reduce NH_4-N loss into the electrode rinse solution, as suggested by van Linden et al. (2019). In addition, the pH of the concentrate should be controlled. During the ED experiments, the concentrate pH remained stable at approximately 8.0–8.3, at which approximately 95 % of TAN lies in the form of NH_4-N. The stable pH range indicates the transport of both NH_4-N and HCO_3^- to the concentrate stream, thus forming a buffered system. Since the remaining 5 % of TAN lies in the volatile NH_3-N form, an alternative approach to enhance recovery and mitigate TAN loss is to lower the pH, shifting the equilibrium towards the non-volatile NH_4-N form.

The NH_4-N current efficiency obtained in both ADLs was in the range of 20 %–50 % in stage 1, and 30 %–55 % in stage 2, which is lower than reported by van Linden et al. (2019) who used synthetic solutions, and owes to the transport of additional ions such as PO_4-P, Ca^{2+} and HCO_3^-. In this study, no steady increase of the PO_4-P concentration in the concentrate was observed, as visible in Fig. S4.

Besides the electricity requirements for the ED process, consisting of the ED unit and pumps, transportation should also be taken into account. A municipal WWTP with a capacity of 300,000 PE lies in a distance of 113 km from WWTP C. For the production of an ED concentrate with a daily load of 440 kg NH_4-N/d (the exact nitrogen demand for WWTP C) and with an NH_4-N concentration of 15 g/L, a concentrate volume of 29.4 m^3 is needed. This concentrate volume corresponds to approximately 29.4 tones, which is suitable to be transported by heavy trucks. To estimate the SEC for transportation, a diesel energy content of 10 kWh/L and a fuel efficiency of 0.2 L/km, typical for large trucks under load, were assumed. By multiplying the energy content and the fuel efficiency, the SEC for transportation is expected to be approximately 0.5 kWh/kg NH_4-N, which is negligible compared to the electricity requirements for the ED unit and comparable to the electricity requirement for pumping in the ED process.

Apart from NH_4-N recovery, also the effect of NH_4-N removal on a municipal WWTP was investigated. Baumgartner et al. (2022) compared different biological treatment methods for ADL by performing COD and Total Nitrogen (N) mass and energy balances based on specific data gained from bench-mark studies and full-scale experiments. To investigate how an ED treatment with MF pre-treatment would impact the overall electricity balance of a large single-stage WWTP with anaerobic sludge stabilization, similar mass and energy balances were performed, based on the same assumptions described by Baumgartner et al. (2022),

e.g. PE-specific COD and nitrogen inflow loads, removal performance, sludge retention time in the activated sludge tank (15 days), aeration efficiency, and a CHP electrical efficiency of 30 %. For the MF step, additional assumptions have been made – a flowrate of 20 m^3/h, an operating pressure of 2 bar, an ADL NH_4-N concentration of 1 g NH_4-N/L and a WWTP size of 300,000 PE. Based on the results of the bench-scale experiments, a removal of 90 % was assumed. The mass and energy balances for the reference plant without ADL side-stream treatment are depicted in the supplementary material (Fig. S5). The results for a model plant with MF and ED in side-stream are presented in Fig. 8.

Due to the reduced nitrogen load in the desalinated ADL that is recirculated back to the main-stream treatment, the model plant with MF and ED in side-stream results in a lower nitrogen load to be nitrified and denitrified in the main-stream AST (3.9 g N/(PE·d) compared to 4.6 g N/(PE·d) in the reference plant). This decreases the aeration demand for nitrification but at the same time increases the potential for higher COD removal in the primary settling tank, from typically 30 % up to 40 %, as less COD is used as electron donor for denitrification. To enhance removal of COD in the primary settling tank, different approaches can be applied, such as increasing the hydraulic retention time (HRT), applying coagulants and flocculants, or introducing an MF step before the AST (Lasaki et al., 2023; Väänänen et al., 2016).

In this new scenario, aeration electricity requirement would decrease from 12.3 kWh/(PE·a) (reference plant) to 10.7 kWh/(PE·a). Diverting more organic matter into the PS raises the COD influent load in the anaerobic digester, which results in higher methane production and greater electricity gain than in the reference plant: 17 kWh/(PE·a) versus 14.3 kWh/(PE·a). Taking in account the overall electricity balance, consisting in this specific case of the PE-specific electricity consumption for aeration in main-stream (10.7 kWh/(PE·a)), for MF (0.04 kWh/(PE·a)) and for ED (5.7 kWh/(PE·a)), and the electricity gain from the produced methane (17 kWh/(PE·a)), a net electricity gain of 0.6 kWh/(PE·a) is obtained. Therefore, the electricity consumed by the MF pre-treatment and ED would be compensated by the electricity gained due to the higher methane production and lower aeration demand in the main-stream treatment. In this evaluation, the potential energy consumption or chemical demand associated with increasing COD removal in the primary settling tank, as well as the additional benefit of using the ED concentrate as an alternative nutrient source to urea, were not accounted for.

5. Conclusions

Bench-scale experiments demonstrated that ED can be successfully applied as an NH_4-N recovery technology from municipal ADLs. The two-stage experimental design, intended to enhance NH_4-N concentration by minimizing forward osmosis and NH_4-N back-diffusion following sequencing batch experiments, achieved NH_4-N concentrations of 10 g/L in stage 1 and 15 g/L in stage 2 across both municipal ADLs.

The NH_4-N flux density fluctuated around 0.5 mol/(m^2·h) in stage 1, and increased significantly in stage 2, reaching 6.5 – 6.6 mol/(m^2·h) in ADL A and 2.8 – 3.1 mol/(m^2·h) in ADL B. A volume increase was observed in the experiments with both municipal ADLs, ranging from 1.1 % – 8.5 % in stage 1. In stage 2, the volume increase was more pronounced, with 32.5 % – 34.5 % in ADL A and 23.5 % in ADL B, primarily due to electro-osmosis driven by the high NH_4-N flux density. NH_4-N current efficiency varied in both municipal ADLs between 20.1 % – 45.4 % and 26.9 % – 41.2 % in stage 1. By comparison, stage 2 showed a slight increase in efficiency of 46.5 % – 54.2 % for ADL A, while ADL B remained at a similar level as stage 1.

The SEC varied between 5 and 12 kWh/kg NH_4-N in experiment A11, increasing to 19 kWh/kg NH_4-N in experiment A12. In experiment A21, the SEC rose to a maximum of 21 kWh/kg NH_4-N, likely due to phenomena such as fouling and/or scaling resulting from the absence of a prior cleaning step, while it dropped to 8.5 kWh/kg NH_4-N in experiment A22. In ADL B, SEC values varied between 7 and 21 kWh/kg NH_4-N in both stages, showing no significant impact of the above-mentioned phenomena on SEC. Taking into account all experiments, the mean SEC amounted to 12.9 kWh/kg NH_4-N. This value lies at a similar range as the Haber-Bosch process and at a lower range than the Bosch-Meiser

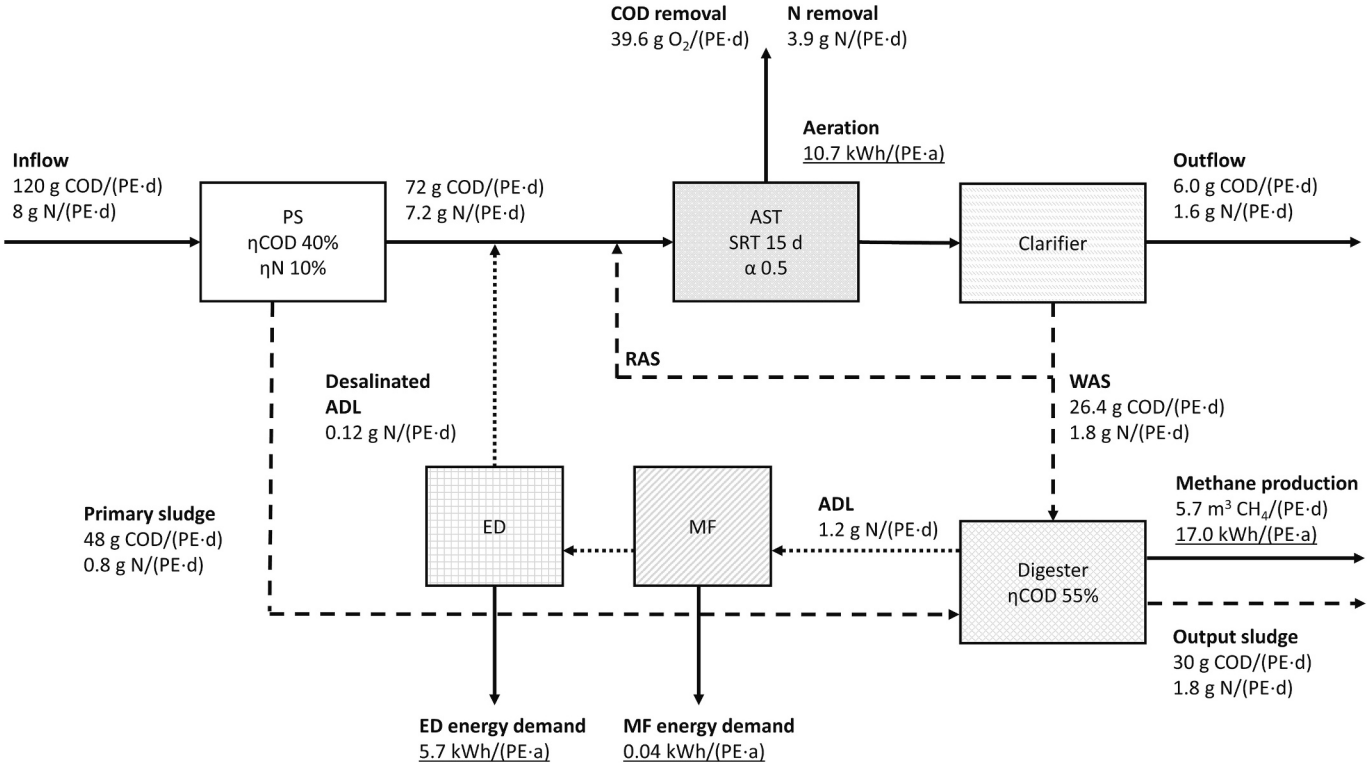

Fig. 8. Proposed COD and nitrogen balance for a single-stage WWTP with MF and ED applied.

process, however, the different energy inputs involved in all processes should be considered to enable comparability.

The large concentration factors obtained suggests that this ED design may also be suitable for a larger municipal WWTP with a sufficient daily NH_4-N load to supply to WWTP C, allowing to potentially replace urea with the ADL concentrate. For the ED operation with a calculated membrane area of 2620 m^2, at least 6 currently commercialized ED units in parallel operation would be required. Since larger flux densities were obtained in stage 2, the membrane area should be reduced in such a parallel operation to maintain the same linear velocity.

In the context of NH_4-N removal from ADL, an ED side-stream treatment with an MF pre-treatment appears to be electrically beneficial in a single-stage WWTP if COD removal in the primary settling tank increases from 30 % to 40 %. This design reduces the electricity demand for aeration while increasing methane production, allowing the electricity consumed by MF and ED to be offset by the electricity gained.

CRediT authorship contribution statement

Liad Weisz: Writing – original draft, Visualization, Methodology, Investigation, Formal analysis, Data curation, Conceptualization. **Daniela Reif:** Writing – review & editing, Methodology, Investigation, Formal analysis, Conceptualization. **Sascha Weilguni:** Methodology, Investigation, Formal analysis, Conceptualization. **Vanessa Parravicini:** Writing – review & editing, Formal analysis, Conceptualization. **Ernis Saracevic:** Writing – review & editing, Validation, Supervision, Project administration, Funding acquisition. **Jörg Krampe:** Writing – review & editing, Validation, Supervision, Project administration, Funding acquisition. **Norbert Kreuzinger:** Writing – review & editing, Validation, Supervision, Resources, Project administration, Funding acquisition, Conceptualization.

Declaration of competing interest

The authors declare that they have no known competing financial interests or personal relationships that could have appeared to influence the work reported in this paper.

Data availability

Data will be made available on request.

Acknowledgment

The authors acknowledge TU Wien Bibliothek for financial support through its Open Access Funding Program.

Appendix A. Supplementary data

Supplementary data to this article can be found online at https://doi.org/10.1016/j.scitotenv.2024.176699.

References

Aguilar-Pozo, V.B., Chimenos, J.M., Elduayen-Echave, B., Olaciregui-Arizmendi, K., López, A., Gómez, J., Guembe, M., García, I., Ayesa, E., Astals, S., 2023. Struvite precipitation in wastewater treatment plants anaerobic digestion supernatants using a magnesium oxide by-product. Sci. Total Environ. 890, 164084. https://doi.org/10.1016/j.scitotenv.2023.164084.

Albornoz, L.L., Marder, L., Benvenuti, T., Bernardes, A.M., 2019. Electrodialysis applied to the treatment of an university sewage for water recovery. J. Environ. Chem. Eng. 7, 102982. https://doi.org/10.1016/j.jece.2019.102982.

Baumgartner, T., Jahn, L., Parravicini, V., Svardal, K., Krampe, J., 2022. Efficiency of Sidestream Nitritation for modern two-stage activated sludge plants. Int. J. Environ. Res. Public Health 19, 12871. https://doi.org/10.3390/ijerph191912871.

Benvenuti, T., Siqueira Rodrigues, M.A., Bernardes, A.M., Zoppas-Ferreira, J., 2017. Closing the loop in the electroplating industry by electrodialysis. J. Clean. Prod. 155, 130–138. https://doi.org/10.1016/j.jclepro.2016.05.139.

Bernardes, A.M., Costa, R.F.D., Fallavena, V.L.V., Rodrigues, M.A.S., Trevisan, M.D., Ferreira, J.Z., 2000. Electrochemistry as a clean technology for the treatment of effluents: the application of electrodialysis. Met. Finish. 98, 52–114. https://doi.org/10.1016/S0026-0576(00)83558-8.

Chen, C., Dai, Z., Li, Y., Zeng, Q., Yu, Y., Wang, X., Zhang, C., Han, L., 2023. Fouling-free membrane stripping for ammonia recovery from real biogas slurry. Water Res. 229, 119453. https://doi.org/10.1016/j.watres.2022.119453.

Gherghel, A., Teodosiu, C., De Gisi, S., 2019. A review on wastewater sludge valorisation and its challenges in the context of circular economy. J. Clean. Prod. 228, 244–263. https://doi.org/10.1016/j.jclepro.2019.04.240.

Han, L., Galier, S., Roux-de Balmann, H., 2015. Ion hydration number and electro-osmosis during electrodialysis of mixed salt solution. Desalination 373, 38–46. https://doi.org/10.1016/j.desal.2015.06.023.

Hyder, A.G., Morales, B.A., Cappelle, M.A., Percival, S.J., Small, L.J., Spoerke, E.D., Rempe, S.B., Walker, W.S., 2021. Evaluation of Electrodialysis desalination performance of novel bioinspired and conventional ion exchange membranes with sodium chloride feed solutions. Membranes 11, 217. https://doi.org/10.3390/membranes11030217.

Jiang, C., Wang, Y., Zhang, Z., Xu, T., 2014. Electrodialysis of concentrated brine from RO plant to produce coarse salt and freshwater. J. Membr. Sci. 450, 323–330. https://doi.org/10.1016/j.memsci.2013.09.020.

Karakatsanis, G., Makropoulos, C., 2022. Resource recovery and the Sherwood plot. Entropy 25, 4. https://doi.org/10.3390/e25010004.

Knežević, K., Reif, D., Harasek, M., Krampe, J., Kreuzinger, N., 2022. Assessment of graphical methods for determination of the limiting current density in complex Electrodialysis-feed solutions. Membranes 12, 241. https://doi.org/10.3390/membranes12020241.

Knežević, K., Daza-Serna, L., Mach-Aigner, A.R., Mach, R.L., Friedl, A., Krampe, J., Kreuzinger, N., 2023. Investigation of ion-exchange membranes and erythritol concentration for the desalination of erythritol culture broth by electrodialysis. Chem. Eng. Process. - Process Intensif. 192, 109494. https://doi.org/10.1016/j.cep.2023.109494.

Kocaturk, I., Erguder, T.H., 2016. Influent COD/TAN ratio affects the carbon and nitrogen removal efficiency and stability of aerobic granules. Ecol. Eng. 90, 12–24. https://doi.org/10.1016/j.ecoleng.2016.01.077.

Lasaki, B.A., Maurer, P., Schönberger, H., 2023. Effect of coupling primary sedimentation tank (PST) and microscreen (MS) to remove particulate organic carbon (POC): a study to mitigate energy demand in municipal wastewater treatment plants. Sustain. Environ. Res. 33, 25. https://doi.org/10.1186/s42834-023-00186-7.

Liu, H., She, Q., 2022. Influence of membrane structure-dependent water transport on conductivity-permselectivity trade-off and salt/water selectivity in electrodialysis: implications for osmotic electrodialysis using porous ion exchange membranes. J. Membr. Sci. 650, 120398. https://doi.org/10.1016/j.memsci.2022.120398.

Liu, R., Wang, Y., Wu, G., Luo, J., Wang, S., 2017. Development of a selective electrodialysis for nutrient recovery and desalination during secondary effluent treatment. Chem. Eng. J. 322, 224–233. https://doi.org/10.1016/j.cej.2017.03.149.

Mao, C., Byun, J., MacLeod, H.W., Maravelias, C.T., Ozin, G.A., 2024. Green urea production for sustainable agriculture. Joule S2542435124001041. https://doi.org/10.1016/j.joule.2024.02.021.

Meng, J., Shi, L., Hu, Z., Hu, Y., Lens, P., Wang, S., Zhan, X., 2022. Novel electro-ion substitution strategy in electrodialysis for ammonium recovery from digested sludge centrate in coastal regions. J. Membr. Sci. 642, 120001. https://doi.org/10.1016/j.memsci.2021.120001.

Mondor, M., Masse, L., Ippersiel, D., Lamarche, F., Massé, D.I., 2008. Use of electrodialysis and reverse osmosis for the recovery and concentration of ammonia from swine manure. Bioresour. Technol. 99, 7363–7368. https://doi.org/10.1016/j.biortech.2006.12.039.

Muscarella, S.M., Badalucco, L., Cano, B., Laudicina, V.A., Mannina, G., 2021. Ammonium adsorption, desorption and recovery by acid and alkaline treated zeolite. Bioresour. Technol. 341, 125812. https://doi.org/10.1016/j.biortech.2021.125812.

Ortiz, J.M., Sotoca, J.A., Expósito, E., Gallud, F., García-García, V., Montiel, V., Aldaz, A., 2005. Brackish water desalination by electrodialysis: batch recirculation operation modeling. J. Membr. Sci. 252, 65–75. https://doi.org/10.1016/j.memsci.2004.11.021.

Papadopoulou, E., González, M.C., Reif, D., Ahmed, A., Tsapekos, P., Angelidaki, I., Harasek, M., 2023. Separation of lactic acid from fermented residual resources using membrane technology. J. Environ. Chem. Eng. 11, 110881. https://doi.org/10.1016/j.jece.2023.110881.

Pastor, L., Mangin, D., Ferrer, J., Seco, A., 2010. Struvite formation from the supernatants of an anaerobic digestion pilot plant. Bioresour. Technol. 101, 118–125. https://doi.org/10.1016/j.biortech.2009.08.002.

Patel, S.K., Biesheuvel, P.M., Elimelech, M., 2021. Energy consumption of brackish water desalination: identifying the sweet spots for Electrodialysis and reverse osmosis. ACS EST Eng. 1, 851–864. https://doi.org/10.1021/acsestengg.0c00192.

Rossi, M., Fanti, O., Pacca, S.A., Comodi, G., 2022. Energy efficiency intervention in urea processes by recovering the excess pressure through hydraulic power recovery turbines (HPRTs). Sustain Energy Technol Assess 52, 102263. https://doi.org/10.1016/j.seta.2022.102263.

Scarazzato, T., Panossian, Z., Tenório, J.A.S., Pérez-Herranz, V., Espinosa, D.C.R., 2018. Water reclamation and chemicals recovery from a novel cyanide-free copper plating bath using electrodialysis membrane process. Desalination 436, 114–124. https://doi.org/10.1016/j.desal.2018.01.005.

Shi, L., Liu, L., Yang, B., Sheng, G., Xu, T., 2020. Evaluation of industrial urea energy consumption (EC) based on life cycle assessment (LCA). Sustainability 12, 3793. https://doi.org/10.3390/su12093793.

Springer, A.M., 1993. Industrial environmental control. Pulp and paper industry. 2nd edition.

Strathmann, H., 2010. Electrodialysis, a mature technology with a multitude of new applications. Desalination 264, 268–288. https://doi.org/10.1016/j.desal.2010.04.069.

Tian, H., Fotidis, I.A., Kissas, K., Angelidaki, I., 2018. Effect of different ammonia sources on aceticlastic and hydrogenotrophic methanogens. Bioresour. Technol. 250, 390–397. https://doi.org/10.1016/j.biortech.2017.11.081.

Tokushige, M., Ryu, J., 2023. Adsorption and Desorption Behaviors of Ammonia on Zeolites at 473 K by the Pressure–Swing Method. ACS Omega 8, 32536–32543. doi: https://doi.org/10.1021/acsomega.3c02882.

Tsiakis, P., Papageorgiou, L.G., 2005. Optimal design of an electrodialysis brackish water desalination plant. Desalination 173, 173–186. https://doi.org/10.1016/j.desal.2004.08.031.

Väänänen, J., Cimbritz, M., la Cour Jansen, J., 2016. Microsieving in primary treatment: effect of chemical dosing. Water Sci. Technol. 74, 438–447. https://doi.org/10.2166/wst.2016.223.

van Linden, N., Spanjers, H., van Lier, J.B., 2019. Application of dynamic current density for increased concentration factors and reduced energy consumption for concentrating ammonium by electrodialysis. Water Res. 163, 114856. https://doi.org/10.1016/j.watres.2019.114856.

Wang, Z., He, P., Zhang, H., Zhang, N., Lü, F., 2022. Desalination, nutrients recovery, or products extraction: is electrodialysis an effective way to achieve high-value utilization of liquid digestate? Chem. Eng. J. 446, 136996. https://doi.org/10.1016/j.cej.2022.136996.

Wang, X., Zhang, X., Wang, Y., Du, Y., Feng, H., Xu, T., 2015. Simultaneous recovery of ammonium and phosphorus via the integration of electrodialysis with struvite reactor. J. Membr. Sci. 490, 65–71. https://doi.org/10.1016/j.memsci.2015.04.034.

Ward, A.J., Arola, K., Thompson Brewster, E., Mehta, C.M., Batstone, D.J., 2018. Nutrient recovery from wastewater through pilot scale electrodialysis. Water Res. 135, 57–65. https://doi.org/10.1016/j.watres.2018.02.021.

Wirthensohn, T., Waeger, F., Jelinek, L., Fuchs, W., 2009. Ammonium removal from anaerobic digester effluent by ion exchange. Water Sci. Technol. 60, 201–210. https://doi.org/10.2166/wst.2009.317.

Xie, M., Shon, H.K., Gray, S.R., Elimelech, M., 2016. Membrane-based processes for wastewater nutrient recovery: technology, challenges, and future direction. Water Res. 89, 210–221. https://doi.org/10.1016/j.watres.2015.11.045.

Yan, H., Xu, C., Li, W., Wang, Y., Xu, T., 2016. Electrodialysis to concentrate waste ionic liquids: optimization of operating parameters. Ind. Eng. Chem. Res. 55, 2144–2152. https://doi.org/10.1021/acs.iecr.5b03809.

Yuan, M.-H., Chen, Y.-H., Tsai, J.-Y., Chang, C.-Y., 2016. Ammonia removal from ammonia-rich wastewater by air stripping using a rotating packed bed. Process. Saf. Environ. Prot. 102, 777–785. https://doi.org/10.1016/j.psep.2016.06.021.

Zeng, L., Mangan, C., Li, X., 2006. Ammonia recovery from anaerobically digested cattle manure by steam stripping. Water Sci. Technol. 54, 137–145. https://doi.org/10.2166/wst.2006.852.